



## **AN INVERSION METHOD TO DETERMINE STRESS DISTRIBUTION ON A FAULT PLANE USING GROUND MOTIONS**

**Hisashi TANIYAMA<sup>1</sup>**

### **SUMMARY**

The rupture process of an earthquake has large effect on near-field ground motions. Because source-time functions are affected by the stress drop process, it is important to understand the dynamic rupture process of earthquake faults to estimate near-field ground motions. Kinematic inversion analyses have been carried out to obtain spatiotemporal slip distributions, from which the stress distributions on the fault plane have been inferred. In this study, an inversion method to infer stress drop process of an earthquake fault is developed. To express a spatiotemporal stress distribution on an earthquake fault during an earthquake, a fault is divided into subfaults and the shear stress on a subfault after the passage of the rupture front is assumed to change repeatedly to its residual stress. Stress changes of subfaults are inferred directly from the observed ground motions. Total rupture processes are composed of the stress change histories of the subfaults. To examine the performance of the method, a simulation test was conducted. A relatively simple model was used in the simulation and the computed synthetics were used as observed seismograms. The inversion was stabilized by adding smoothing constraints and ABIC was employed to objectively determine the optimal values of hyperparameters. The inferred time histories of stress changes on subfaults fit generally well with the assumed rupture process.

### **INTRODUCTION**

Detailed information about dynamic rupture processes of large earthquakes is significant for the precise prediction of strong ground motions. Kinematic inversion analyses have been carried out to obtain spatiotemporal slip distributions, from which the stress distributions and the constitutive relation between slip and stress on the fault plane have been inferred (e.g., Quin [1], Miyatake [2], Fukuyama and Mikumo [3], Ide and Takeo [4][5], Day et. al. [6], Mikumo et. al. [7]).

In kinematic waveform inversions, a fault is usually divided into subfaults and time histories of displacement at subfaults are inferred. With a proper modification, the method used in kinematic waveform inversions can be used to infer a spatiotemporal stress distribution from observed waveforms.

In this study, an inversion method to infer stress drop process of an earthquake fault is developed. A simulation test was conducted to examine the performance of the method.

---

<sup>1</sup> Research Associate, Saitama University, Saitama, Japan

## METHOD

### Stress distribution on a fault plane

The goal of this study is to present and examine the inversion method to determine a spatiotemporal stress distribution on an earthquake fault. Toward this goal, like inversion method commonly used in kinematic waveform inversion analyses, a fault plane is divided into subfaults and the time history of stress on each subfault is inferred. Once we obtain the stress acting on a fault as a function of time and position, we can reconstruct the dynamic rupture process of the earthquake and the relation between stress and slip can be obtained.

In linear elastodynamics, seismic waves are sensitive to stress change and insensitive to absolute stress level. Thus in this study, only stress changes are dealt with, i.e., we assume  $\tau_0$  (initial stress) = 0. Accordingly the displacement is measured from the state at  $t = 0$ .

To express a stress change history, the shear stress at a point on a fault surface after the passage of the rupture front is assumed to change repeatedly to its residual stress (Fig. 1).

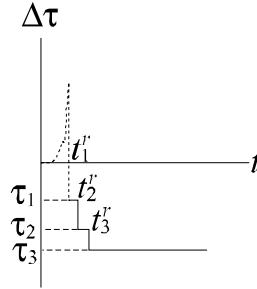


**Figure 1. Assumed stress change history.**

Shear stress before the rupture is calculated based on the theory of linear elasticity. This stress change history is expressed as

$$\Delta \tau = \mu \left( \frac{\partial u_s}{\partial x_n} + \frac{\partial u_n}{\partial x_s} \right) \quad (\text{if } t < t_1^r) \quad (1)$$

and

$$\Delta \tau = \phi(t) \quad (\text{if } t \geq t_1^r) \quad (2)$$

where  $t_1^r$  is the time of the passage of the rupture front,  $\mu$  is the Lamé modulus. 'n' indicates the direction normal to the fault plane. The shear stress considered in equation (1) and (2) is assumed to act in the direction of 's'.  $\phi(t)$  in equation (2) is a function of time that satisfies the following equation

$$\phi(t) = \tau_k \quad (t_k^r \leq t < t_{k+1}^r) \quad (3)$$

where  $t_k^r$  is the time when the  $k$ th stress change occurs.

As shown in Fig. 2,  $\phi(t)$  can be expressed as the sum of the functions  $\varphi_k(t)$ , representing unit stress drop at  $t = t_k^r$ .

$$\phi(t) = \sum_{k=1}^K a_k \varphi_k(t) \quad (4)$$

where  $K$  is the total number of stress changes. The expansion coefficients  $a_k$  in equation (4) indicate the stress drop at  $t = t_k^r$  and are given by

$$a_1 = -\tau_1 \quad (5)$$

$$a_k = \tau_{k-1} - \tau_k \quad (k \geq 2) \quad (6)$$

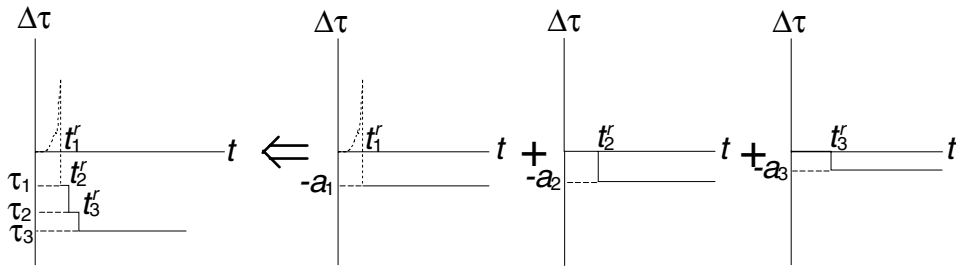


**Figure 2. Division of the stress drop process.**

To infer a spatial distribution of stress, a fault is divided into subfaults. If each subfault is expressed as a crack on which the stress drop occurs, the displacement at the edge of the subfault is 0 and the stress near the tip of the subfault becomes high. If we sum up these displacements and stresses, the resultant displacement and stress distribution may be different from the one on the actual fault surface. Therefore, the following conditions are imposed on the assumed fault and subfaults.

$$\Delta \tau(\xi) = \mu \left( \frac{\partial u_s}{\partial x_n} + \frac{\partial u_n}{\partial x_s} \right) \quad (\text{if } t < t_1^r(\xi)) \quad (7)$$

$$\Delta \tau(\xi) = \varphi_k(t, \xi) \quad (\text{if } t \geq t_1^r(\xi) \text{ and } \xi \text{ is on the subfault}) \quad (8)$$

$$\Delta \tau = 0 \quad (\text{if } t \geq t_1^r(\xi) \text{ and } \xi \text{ is outside the subfault but on the fault plane}) \quad (9)$$

where  $\xi$  is a point on the fault surface.

### Inversion method

Once we calculate the waveform ( $u_{ijk}(t)$ ) at the  $i$ th station generated by  $\varphi_{jk}(t)$  (i.e., unit stress drop on the  $j$ th subfault at  $t = t_k^r$ ), then the  $i$ th synthetic seismogram  $u_i(t)$  is given by the summation of  $u_{ijk}(t)$  multiplied by the stress drop ( $a_{jk}$ ) on the  $j$ th subfault at  $t = t_k^r$ .

$$u_i(t) = \sum_{j,k} a_{jk} u_{ijk}(t) \quad (10)$$

The  $i$ th observed record is expressed by the discrete time series of  $O_i(t_l)$ ,  $l = 1, L$ , where  $L$  is the total number of time points for the record. The equation with observed waveform  $O_i(t_l)$  is expressed as

$$O_i(t_l) = u_i(t_l) + e_i(t_l) = \sum_{jk} a_{jk} u_{ijk}(t_l) + e_i(t_l) \quad (11)$$

where  $e_i(t_l)$  is the error between the observed and synthetic seismogram.  $a_{jk}$ ,  $j=1, J$  and  $k=1, K$  are the model parameters to be determined. Here  $J$  is the total number of subfaults. In inferring the model parameters  $a_{jk}$ , along with equation (11), smoothing constraints are added to reduce instability and repress excessive variances in model parameters. Based on the presumption that stress changes close together in space and in time should be similar, two constraints (i.e., the temporal constraint and the spatial constraint) are assigned. In addition to the above smoothing constraints, the condition that final displacements on all subfaults are nonnegative is imposed. Parameters that minimize the error in equation (11) and in the smoothing constraints satisfying the nonnegative condition are inferred by least squares (Lawson and Hanson [8]). The optimal values of hyperparameters that control the strength of the smoothing constraints are determined objectively based on Akaike's Bayesian information criterion (ABIC) (Akaike [9], Yabuki and Matsu'ura [10], Ide and Takeo [6]).

## MODEL

To examine the performance of the inversion method, a simulation test was performed. First, strong ground motions were computed with an assumed model. The computed waveforms were used as "observed seismograms". The object of the simulation was to test if the assumed rupture process could be reproduced by the inversion method. Relatively simple model was used. P wave velocity, S wave velocity and the density of the medium were assumed to be 6.1 km/s, 3.5 km/s and 2.6 g/cm<sup>3</sup>, respectively. Fig. 3 shows the geometry of the simulation model.

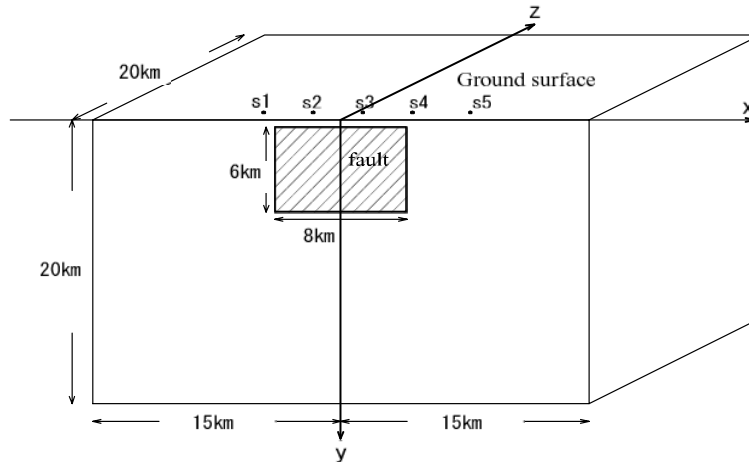


Figure 3. Geometry of the model.

The fault was assumed to be a strike-slip fault. Its surface was represented with a vertical plane whose length and width were 8 km and 6 km respectively, and was placed at depths  $6.5 \text{ km} \geq y \geq 0.5 \text{ km}$  on  $z = 0$  plane. Because of the symmetry with respect to the  $z = 0$  plane, waveforms were calculated only in  $z \geq 0$ . The following equations were solved by finite difference method (Virieux and Madariaga[11]).

$$\rho \dot{v}_i = \sigma_{ij,j} \quad (12)$$

$$\dot{\sigma}_{ij} = \lambda v_{k,k} \delta_{ij} + \mu (v_{i,j} + v_{j,i}) \quad (13)$$

where  $\rho$  is the density of the medium,  $\sigma_{ij}$  is the  $ij$  component of the (incremental) stress,  $\lambda$  and  $\mu$  are the Lamé moduli,  $v_k$  is the  $k$  component of the velocity and  $\delta_{ij}$  is Kröncher's delta. Dots indicate time derivatives, commas partial differentiation with respect to the space component indicated by the index following comma. The intervals of the staggered grids and time were 250m and 0.02s respectively.

The fault plane was divided into twelve  $2\text{km} \times 2\text{km}$  areas (Fig. 4).

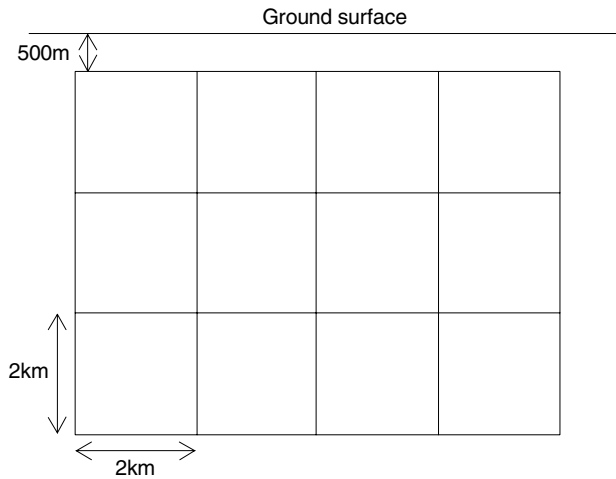


**Figure 4. Division of the fault surface.**

In the analysis to compute the “observed waveforms”, the same time history of stress change was used at every point in each divided area as shown in Fig. 5. Only the stress changes of the shear stress that exerts in the strike direction of the fault were considered in the simulation. In Fig. 5, twelve rectangles indicate the divided  $2 \text{ km} \times 2 \text{ km}$  areas and the stress change history within each area is shown. The stress before the passage of the rupture front was computed by equations (12) and (13), thus it is not shown in Fig. 5. In some areas, the stress was assumed to change repeatedly to its residual stress and the intervals of stress changes were 0.25 s to 0.3 s. In the other areas, the stress drop was assumed to occur in 1 time step.

The velocity waveforms computed at 5 points (stations) shown in Fig. 3 were used as “observed seismograms”. The “observed seismograms” were lowpass filtered (1.2Hz) to eliminate the effect caused by the dispersive property of the finite difference method.

In the inversion analysis, twelve  $2\text{km}\times 2\text{km}$  areas were used as subfaults. The shear stress on each subfault was assumed to change when the rupture front passes and also at 0.33s and 0.66s after the passage of the rupture front (3 times in total). A rupture front was assumed to propagate from the subfault denoted by a star in Fig. 5 at a constant velocity, i.e., the subfault where the rupture started was assumed to be known. Assigning various rupture velocities, inversion analyses were carried out. Among the sets of parameters inferred according to the assigned rupture velocity, the parameters that minimized the error in equation (11) were chosen as the final solution.

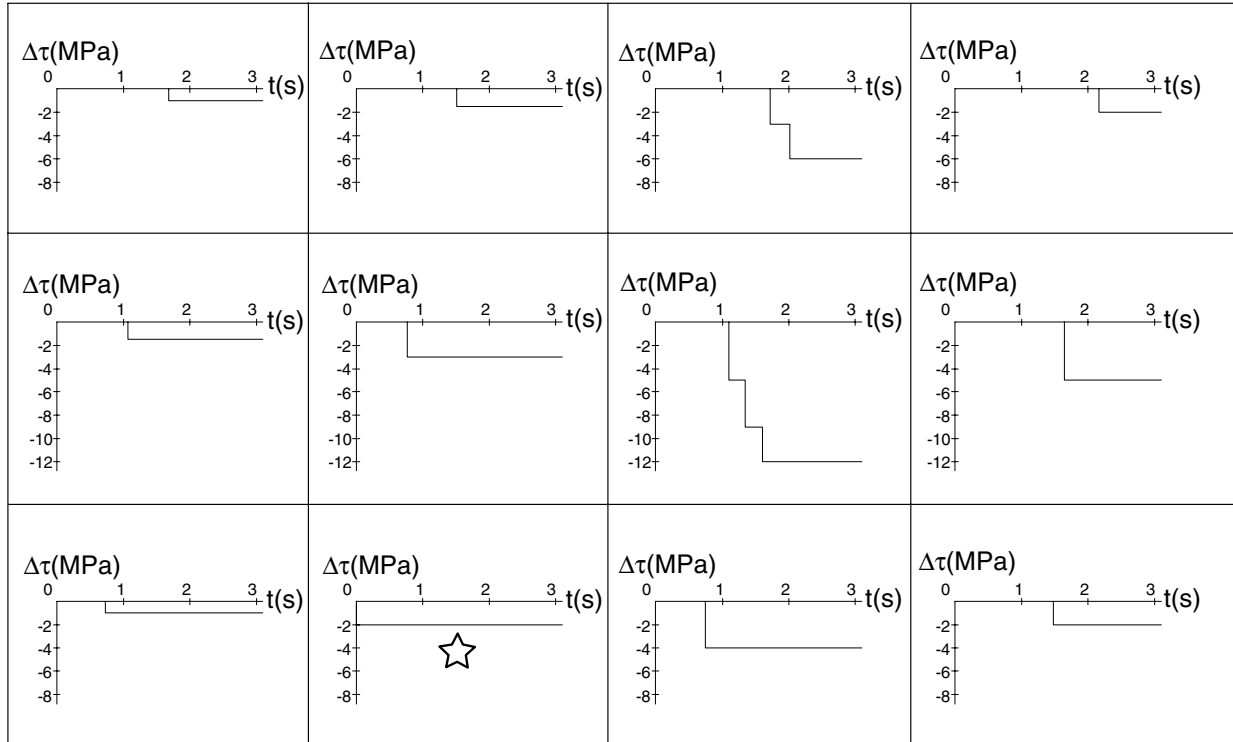


**Figure 5. Stress change histories assumed in computing “observed seismograms”. Twelve rectangles indicate the divided  $2\text{km}\times 2\text{km}$  areas. A star denotes the area where the rupture starts.**

## RESULTS AND DISCUSSION

Fig. 6 shows the result of the inversion analysis. Twelve rectangles indicate the subfaults. Solid lines and dotted lines denote the inferred time histories of stress changes and the time histories used in computing the “observed seismograms” respectively. The inversion result in the shallow area and the area where the stress drop is high matches the assumed stress change history fairly well, whether the stress drop occurs in 1 time step or the stress changes repeatedly. On the other hand, the fit in deep areas where small stress change was assigned is worse. The stress on the subfault that has relatively larger effect on the “observed seismogram” was inferred fairly well, while the inversion result of the subfault that has less effect on the “observed wave” was not good.

Fig. 7 shows the comparison of the synthetic waveforms computed based on the inferred result to the “observed seismograms” at 5 stations in Fig. 3. Both synthetics and “observed seismograms” are lowpass filtered (1.2Hz). In either station, all 3 components of the synthetic waveforms give a good fit to the “observed seismograms”. The overall characteristics of the assumed model could be inferred by the inversion method. The inversion method presented in this study can reproduce the stress change history on

a fault plane, provided that precise subsurface structures, fault location and seismograms are obtained and that the station distribution is good. These conditions would be too ideal for the practical inversion analysis and the investigation regarding the resolution and the stability of the solution will be needed to apply this inversion method in practice.

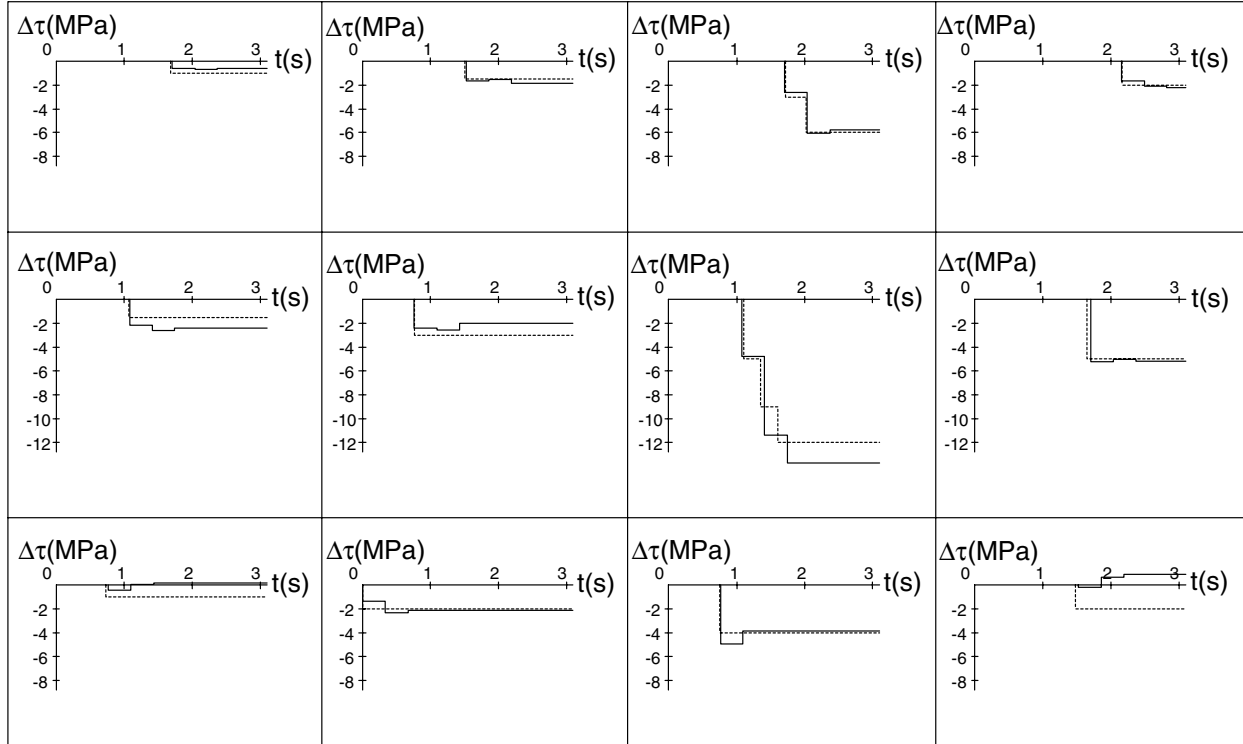


**Figure 6. The result of the inversion analysis. Solid lines indicate the inferred time history of stress changes on each subfault. Dotted lines denote the assumed history in computing the “observed seismograms”.**

## CONCLUSIONS

An inversion method has been developed to determine the stress distribution on a fault surface from observed ground motions. In this method, the earthquake fault is divided into subfaults and the shear stress on a subfault after the passage of the rupture front is assumed to change repeatedly to its residual stress. The spatiotemporal stress distribution on an earthquake fault is determined by the least squares inversion imposing smoothing constraints and the condition that the final displacement on each subfault is nonnegative. ABIC is employed to objectively determine the strength of the smoothing constraints. The performance of the inversion method has been examined by a numerical simulation test. A relatively simple model was assumed in the simulation. The overall characteristics of the assumed stress distribution have been successfully reproduced by the inversion analysis. Although the investigation regarding the resolution and the stability of the solution will be needed to apply this method to practical analyses of real earthquakes, the validity of the inversion method with respect to the simple model has been confirmed.

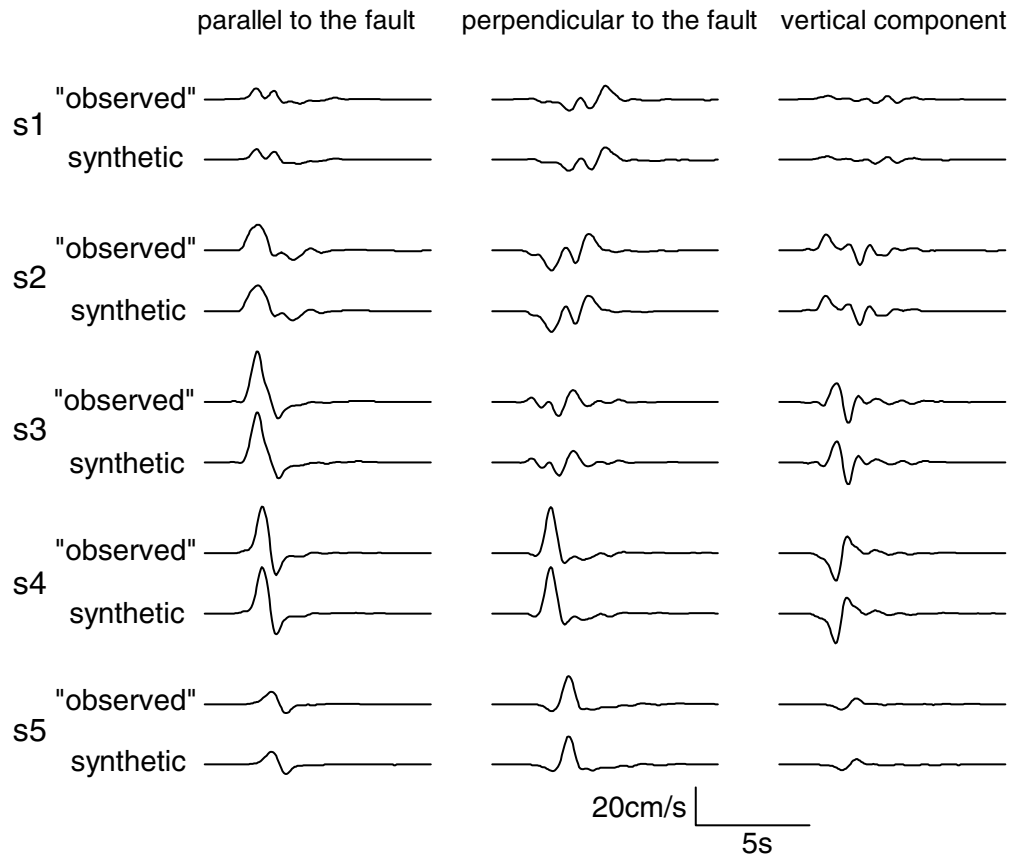


**Figure 7. Comparison of the synthetics to the “observed seismograms”.**

## REFERENCES

1. Quin H. “Dynamic stress drop and rupture dynamics of the October 15 1979 Imperial valley California earthquake”, *Tectonophysics*, 1990, 175: pp. 93-117.
2. Miyatake T. “Reconstruction of dynamic rupture process of an earthquake with constraints of kinematic parameters”, *Geophys. Res. Lett.*, 1992, Vol.19, No.4: pp. 349-352.
3. Fukuyama E. and Mikumo T. “Dynamic rupture analysis: Inversion for the source process of the 1990 Izu-Oshima Japan earthquake (M=6.5)”, *J. Geophys. Res.*, 1993, Vol. 98, No. B4: pp. 6529-6542.
4. Ide S. and Takeo M. “The dynamic rupture process of the 1993 Kushiro-oki earthquake”, *J. Geophys. Res.*, 1996, Vol. 101, No. B3: pp. 5661-5675.
5. Ide S. and Takeo M. “Determination of constitutive relation of fault slip based on seismic wave analysis”, *J. Geophys. Res.*, 1997, 102: pp. 27379-27391.
6. Day S. M., Yu G. and Wald D. J. “Dynamic stress changes during earthquake rupture”, *Bull. Seism. Soc. Am.*, 1998, Vol. 88, No. 2: pp. 512-522.
7. Mikumo T., Olsen K. B., Fukuyama E. and Yagi Y. “Stress-breakdown time and slip-weakening distance inferred from slip-velocity functions on earthquake faults”, *Bull. Seism. Soc. Am.*, 2003, Vol. 93, No. 1: pp. 264-282.
8. Lawson C. L. and Hanson R. J. “Solving least squares problems” SIAM, 1995. (an unabridged, revised republication of the work first published by Prentice-Hall, 1974)
9. Akaike H. “Likelihood and the Bayes procedure”, *Bayesian Statistics* (Bernardo J. M., De Groot M. H., Lindley D. V. and Smith A. F. M., eds.), University Press, Valencia, Spain, 1980: pp. 143-166.

10. Yabuki T. and Matsu'ura M. "Geodetic data inversion using a Bayesian information criterion for spatial distribution of fault slip", *Geophys. J. Int.*, 1992, 109: pp. 363-375.
11. Virieux, J. and Madariaga R. "Dynamic faulting studied by a finite difference method", *Bull. Seism. Soc. Am.*, 1982, 72: pp. 345-369.